Two-Dimensional ^{1}H NMR Studies of Synthetic Immobile Holliday Junctions

Shiow-meei Chen, Fred Heffron, Werner Leupin,‡ and Walter J. Chazin*

Department of Molecular Biology, Scripps Clinic and Research Foundation, 10666 North Torrey Pines Road, La Jolla, California 92037

Received September 7, 1990; Revised Manuscript Received November 7, 1990

ABSTRACT: Two 32 base pair, four-arm immobile Holliday junctions have been prepared and studied by two-dimensional ^{1}H nuclear magnetic resonance (NMR) spectroscopy. Two-quantum spectroscopy provides scalar (through bond) correlations for the 1′H, 2′H, and 2″H resonances of the deoxyribose sugar rings and the nonlabile cytosine and thymine base protons. Assignments in the deoxyribose sugars are extended to the 3′H resonances principally from relayed connectivities in total correlation spectra. Severe overlap of resonances in the standard regions of two-dimensional nuclear Overhauser enhancement (NOE) spectra necessitated the use of a unique approach for obtaining sequence-specific assignments of duplex DNA, wherein all possible NOE connectivities in the spectra are analyzed. These studies of 64-residue structures represent a substantial step forward with respect to the size of oligonucleotide for which virtually complete assignments are obtained. The assignments form the critical background for the detailed analysis of Holliday junction structure and dynamics that is required to address key issues in understanding the role of Holliday junctions in genetic recombination and repair.

A specific DNA structure, the Holliday junction (Holliday, 1964), is an intermediate in all recombination and many repair processes in the cell. A large body of evidence has been gathering that appears to indicate that HJs[1] play an important role in determining the outcome of these genetic events. For example, it has been known for some time that the DNA sequence at or near the junction has an influence on the way in which the Holliday junction is resolved by HJ-cleaving enzymes; e.g., the ratio of (parental to recombinational) products varies with the gene (Whitehouse, 1982). Recently, it has been reported that the structure of the HJ is very sensitive to the DNA sequence at the junction [e.g., Duckett et al. (1988), Parsons et al. (1989), and Mueller et al. (1990)]. These results may have important biological implications, as they appear to parallel the sequence-dependent differences in resolution by the cells' recombination machinery.

HJs are inherently mobile structures; the property of branch migration is critical to the generation of recombined products. Structurally heterogeneous systems such as HJs are notoriously difficult to study by physical methods. Seeman, Kallenbach, and co-workers proposed the study of model synthetic *immobile* HJs to obtain information about the molecular details of these structures (Seeman, 1982; Seeman & Kallenbach, 1983). Several laboratories subsequently reported that immobile HJs have retarded electrophoretic mobilities [e.g., Gough and Lilley (1985)]. The degree of retardation has been correlated with the average branch angles of the HJ (Cooper & Hagerman, 1987; Duckett et al., 1988). From analysis of the imino proton portion of the ^{1}H NMR spectrum of a 32 base pair, four-arm immobile junction, it was concluded that all bases, up to and including the junction, are paired (Wemmer et al., 1985). This is consistent with an analysis of the CD spectrum (Marky et al., 1987) and with studies using chemical probes (Gough et al., 1986; Furlong & Lilley, 1986). In subsequent studies, an immobile HJ was reported to be a 2-fold symmetric structure, in which the arms form two stacking domains with arm I stacking on arm II and with arm III on arm IV (Churchill et al., 1988; Mueller et al., 1988). Recently, fluorescence energy transfer observed in synthetic immobile HJs has been interpreted in terms of a right-handed noncrossed antiparallel X structure (Murchie et al., 1989).

More detailed knowledge of the three-dimensional structure of HJs is clearly of interest and should provide important insights into understanding how the sequence at the junction influences HJ structure and the interaction with HJ-resolving enzymes and why the cells' recombination machinery is influenced by sequence. We report here on our progress with 2D ^{1}H NMR to study the three-dimensional structure and dynamics of 32 base pair synthetic immobile HJs.

The critical first step in any detailed analysis by NMR spectroscopy is the assignment of resonances to specific atoms in the molecule. Methods for sequence-specific assignment of the ^{1}H resonances of small duplexes were worked out almost 10 years ago and are now routinely applied to the study of duplexes in the range of 10–16 base pairs [reviewed in Wemmer and Reid (1985), Wüthrich (1986), Patel et al. (1987), Reid (1987), and van de Ven and Hilbers (1988)]. The largest molecule to be completely assigned to date is a non-self-complementary 23 base pair duplex (Otting et al., 1987; Grütter et al., 1988). The study of a 32 base pair DNA structure presents a very formidable problem for detailed study by ^{1}H NMR spectroscopy. This report demonstrates how the challenges of assigning the ^{1}H NMR spectra of the nonlabile protons of 32 base pair HJs are being met.

Materials and Methods

The seven oligonucleotide strands required for preparation of J1 and J2 (Figure 1) were each synthesized on a 10-μmol

‡ Present address: F. Hoffmann LaRoche, Ltd., Basel, Switzerland.

[1] Abbreviations: HJ, Holliday junction; CD, circular dichroism; UV, ultraviolet; NMR, nuclear magnetic resonance; 1D, one dimensional; 2D, two dimensional; COSY, correlated spectroscopy; 2Q, two-quantum spectroscopy; TOCSY, total correlation spectroscopy; NOE, nuclear Overhauser effect; NOESY, 2D NOE spectroscopy; EDTA, ethylenediaminetetraacetic acid; PAGE, polyacrylamide gel electrophoresis; Tris, tris(hydroxymethyl)aminomethane; d_i(A;B), intranucleotide distance between protons A and B; d_s(A;B), sequential distance between protons A and B, where A is in the 5′ direction relative to B.

0006-2960/91/0430-766$02.50/0 © 1991 American Chemical Society

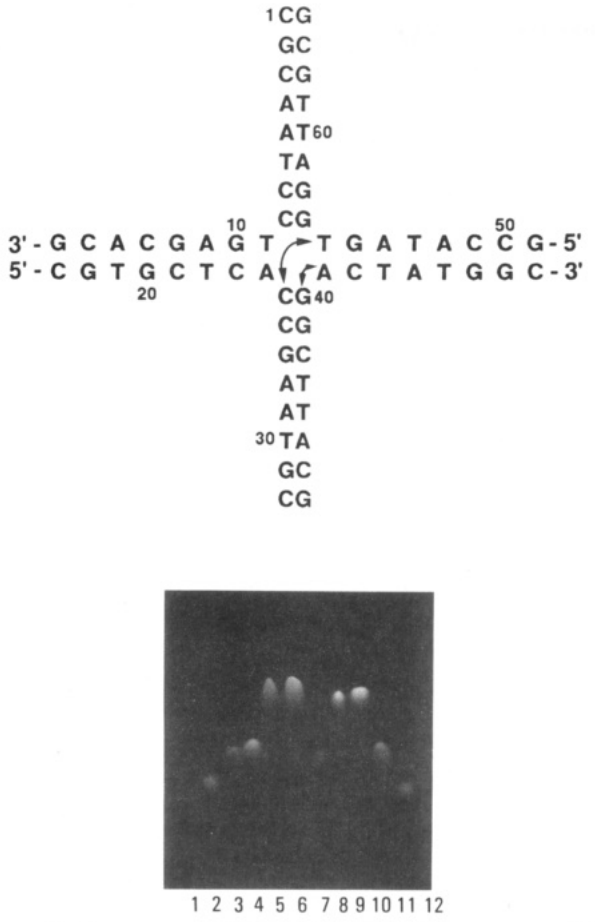

FIGURE 1: Sequence and PAGE of J1 and J2. The sequence of J1 is shown in the upper panel. The sequence of J2 is indicated by the arrows; the C25–G40 and A41–T56 base pairs in J1 exchange places, becoming T25–A40 and G41–C56 base pairs in J2. In the lower panel, the gel lanes contain the following: (1, 2, 11, and 12) single strands; (3, 4, 7, and 10) pairs of half-complementary strands; (5 and 6) two loadings of J1; (8 and 9) two loadings of J2. Samples containing 0.01 A^{260} unit were applied to a 20% polyacrylamide gel and run at constant voltage for approximately 20 h in buffer containing 89 mM Tris base, 89 mM boric acid, and 2 mM Na_2EDTA. The bands were visualized by soaking the gels in 0.25 mM ethidium bromide.

scale by solid-phase β-cyanoethyl phosphoramidite techniques on an Applied Biosystems 380B DNA synthesizer. After deblocking, the strands were purified by DEAE-Sephacel (Pharmacia) chromatography with a linear gradient of 0.3–0.8 M triethylamine bicarbonate at pH 7.0. The purified oligonucleotides were dialyzed against 4 M NaCl to bring the strands into the sodium form and then further dialyzed against H_2O, lyophilized, and redissolved in 400 μL of H_2O. The approximate concentration of each strand was determined by UV absorption. The half-complementary strands 1 and 2 were mixed together and examined at 75 °C by ^{1}H NMR. The resulting solution was titrated to within a few percent of 1:1 by comparison of peak intensities. A second solution containing strands 3 and 4 was prepared in the same manner. These two solutions were then lyophilized and redissolved in stock buffer [20 mM Tris-d_{11} (MSD Isotopes, Montréal, Canada) at pH 7.5, 50 mM NaCl, 5 mM $MgCl_2$, 0.2 mM EDTA, 0.1% NaN_3]. The amount of each solution required to give a 1:1:1:1 ratio was determined by a series of titrations on overload polyacrylamide gels, since the strands, half-complementary duplexes, three-arm structures, and HJs all have different mobilities (Figure 1). The NMR samples were prepared by lyophilizing the resultant 1:1:1:1 solutions and then redissolving them in 420 μL of 95% H_2O/5% ^2H_2O, giving a strand concentration of 1 mM. The HJs were annealed by heating the solution in the NMR tube to 90 °C in a water bath and then slowly cooling to room temperature. The ^{2}H-exchanged samples were prepared by repeated lyophilization from ^2H_2O, followed by dissolution in 99.996% H_2O (MSD Isotopes, Montréal, Canada).

NMR experiments were performed with a Bruker AM-600 spectrometer equipped with an Aspect 3000 computer. All spectra were acquired and plotted in the phase-sensitive mode. The standard pulse sequence and phase cycling were used for 2Q spectra (Braunschweiler et al., 1983) with a composite 180° pulse (Levitt & Freeman, 1979). The transmitter was placed to the low-field side of the C1′ protons, and the correlations to the 5H and $5CH_3$ resonances were folded in the ω_1 dimension. A total of 96 scans/t_1 value were acquired with a 30-ms preparation period and t_{1max} = 26 ms. TOCSY (Braunschweiler & Ernst, 1983; Bax & Davis, 1985) spectra were acquired by use of the modifications described by Rance (1987) with DIPSI-2 (Shaka et al., 1988) mixing for 52 ms, 64 scans/t_1 value, and t_{1max} = 43 ms. The standard pulse sequence was utilized for NOESY spectra (Macura & Ernst, 1980). For the H_2O spectra, the last pulse was replaced by a jump-and-return composite pulse (Plateau & Gueron, 1982), and no other means of solvent suppression was necessary. A total of 96 scans/t_1 value were acquired with a 190-ms mixing time, t_{1max} = 22 ms, and the excitation sequence adjusted to give a maximum just to the high-field side of the imino protons. For the ^2H_2O spectra, the residual HOD was saturated during the preparation period and the mixing time, and a short Hahn-echo period was included to improve the quality of the baseline [e.g., Davis (1989)]. A total of 96 scans/t_1 value were acquired with a 100-ms mixing time and t_{1max} = 37 ms. For the TOCSY and NOESY spectra, the transmitter was placed on the solvent resonance, and the TPPI method was used to achieve quadrature phase detection in the ω_1 dimension (Marion & Wüthrich, 1983). The data were processed on a CONVEX C240 computer with FTNMR software (Hare Research, Inc., Woodinville, WA).

Results

The two 32 base pair, four-arm Holliday junctions selected for detailed analysis are shown in Figure 1. J1 has been extensively studied by Seeman, Kallenbach, and co-workers and provided a baseline for our studies to establish methods for preparation, handling, and characterization of HJs. For example, CD measurements for J1 closely match the published results (Marky et al., 1987). J2 is a simple permutation of J1, with an exchange between branches 3 and 4 of the base pairs at the junction as indicated in Figure 1. These two junctions have different mobilities on polyacrylamide gels (Figure 1) and slightly different T_m values, evidence that they have different structures.

It is important to establish the conformation type and optimal conditions for NMR experiments in order to assign the ^{1}H NMR spectrum with confidence. Measurements of UV absorption [λ_{max} = 258 nm; no shoulder near 295 nm], CD [λ_{max} near 280 nm with positive ellipticity and isoelliptic point at 265 nm], and the ^{31}P NMR spectrum [all resonances in a very narrow (~1 ppm) bandwidth] all indicate that J1 and J2 contain a very large proportion of right-handed, double-stranded helix, presumably in the B-type family. Chemical shifts of the nonlabile protons did not vary significantly in 1D ^{1}H NMR spectra recorded in the temperature range 4–37 °C, which indicates that the structure remains intact over this full range and that spectral analysis can be carried out at any temperature in this range.

The sequence-specific assignment of the ^1H resonances of oligonucleotides proceeds in two stages. First, the spin systems of the cytosine and thymine bases and of the sugar ring protons are identified in experiments which generate information based on scalar (through bond) couplings (e.g., COSY, TOCSY, and 2Q). The corresponding base and sugar protons for each nucleotide are then matched and the sequentially adjacent nucleotides identified, in experiments that generate information based on dipolar (through space) coupling (NOESY). This protocol has been extensively discussed in the literature [e.g., Wemmer and Reid (1985), Wüthrich (1986), Patel et al. (1987), Reid (1987), and van de Ven and Hilbers (1988)]. In the following sections, the general applicability of this approach is demonstrated for the 32 base pair HJs. The particular techniques that could be successfully utilized to study these molecules are identified, along with the connectivities within these spectra that were most useful for obtaining the assignments.

Spin System Identification. The relatively large size of J1 and J2 results in line widths that are significantly greater than those observed for the 10–20-mers that have been previously studied by 2D ^1H NMR. One consequence of these large line widths is that COSY, the usual experimental method for identifying scalar correlation, does not work well for HJs as a result of self-cancellation of the double antiphase cross peaks. However, the corresponding scalar correlations can be observed in 2Q spectra because the peaks have in-phase multiplet structure in the ω_1 dimension. Although TOCSY spectra are even less sensitive to the scalar coupling constant to line width ratio because the cross peaks are in-phase in both dimensions, we find that 2Q is often the method of choice for analyzing direct scalar correlations for J1 and J2, vide infra; in spectral regions that are very crowded (as invariably found for HJs), cross peaks tend to merge in TOCSY spectra, whereas the antiphase multiplet structure in the ω_2 dimension of 2Q spectra provides superior resolution of individual peaks.

In the present study, the identification of scalar correlations was broken down into four separate stages, corresponding to the assignment of four groups of connectivities that could be readily identified. The first of these is the cytosine 5H–6H connectivities. Figure 2A shows a region of the 600-MHz 2Q spectrum of J1 acquired at 310 K. It contains the ω_1 = 5H + 6H, ω_2 = 5H direct peaks that identify the 5H and 6H resonance frequencies for 18 of the 19 cytosine residues. In fact, only 17 discrete peaks are observed in this plot, because the peaks for C32 and C34 are overlapped at ω_1 = 12.94 ppm, ω_2 = 5.47 ppm. The corresponding peaks in the complementary ω_1 = 5H + 6H, ω_2 = 6H region of the spectrum (not shown) are resolved. No 2Q signal is obsrved for the 19th residue, C25 (at the junction), because the line widths for the H5 and H6 resonances are substantially larger than those for the other cytosine residues in the molecule. The resonance pair for C25 could only be identified in the NOESY spectra. The 2Q spectrum of J2 provides very similar results. The direct peak that is broadened beyond detection in J2 is from residue 56, rather than residue 25, due to the exchange of the base pairs at the junction.

The second set of scalar connectivities that could be analyzed in the 2Q spectra were for the $5CH_3$ and 6H resonances of thymines. The ω_1 = $5CH_3$ + 6H, ω_2 = $5CH_3$ direct peaks are located in a charactristic region of the spectrum, and from these, 12 of the 13 sets of resonances were identified for J1 and J2. As for the cytosines, the signals for certain thymine residues at the junction [T56(J1), T25(J2)] were substantially broader than the rest, and the resonance frequencies could only be identified in NOESY spectra.

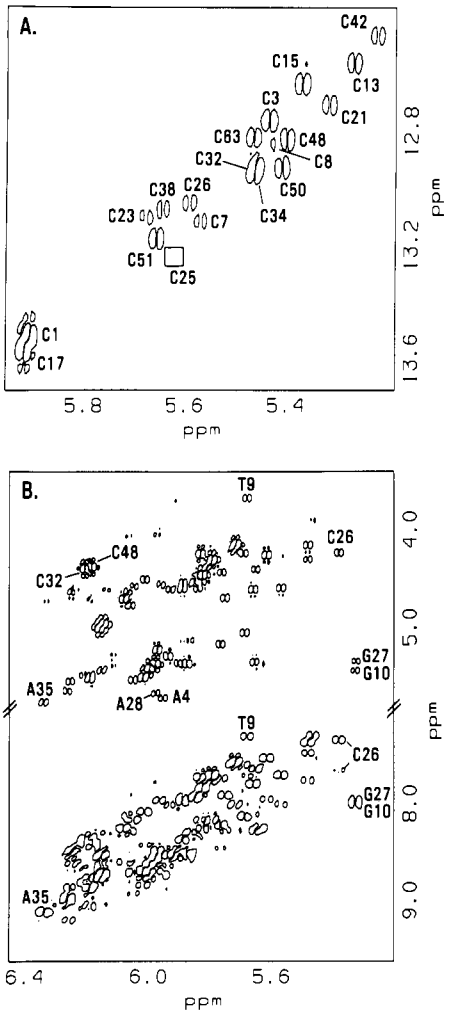

FIGURE 2: Spectral regions of 600-MHz 2Q spectra of 1 mM J1 acquired with a 30-ms excitation period at 37 °C. The buffer contained 20 mM Tris-d_{11}, 50 mM NaCl, 5 mM $MgCl_2$, 0.2 mM EDTA, and 0.1% (w/v) NaN_3, and the pH was adjusted to 7.5. (A) The ω_1 = 5H + 6H, ω_2 = 5H direct peaks, labeled with the sequence-specific assignments. A box is drawn at the location of the peak for C25, although it is broadened beyond detection at this temperature. (B) Spectral region showing the ω_1 = 1′H + 2′H, 1′H + 2″H, ω_2 = 1′H direct peaks (lower panel) and the ω_1 = 2′H + 2″H, ω_2 = 1′H remote peaks (upper panel). A selection of peaks are highlighted by labeling with their sequence-specific assignment. G10 and G27 are discussed in the text. C26 is an example where all three expected peaks are observable. These and A4, T9, A28, and A35 have uniquely shifted 1′H, 2′H, and 2″H resonances. The C32 and C48 peaks are characteristic of 3′-terminal cytosines.

The third set of connectivities analyzed in the 2Q spectra were those identifying the 1′H–2′H–2″H spin *sub*systems of the sugar rings. Three connectivities are expected at ω_2 = 1′H for each of the 64 sugar rings, corresponding to direct peaks at ω_1 = 1′H + 2′H and ω_1 = 1′H + 2″H and remote peaks at ω_1 = 2′H + 2″H. The direct and remote peak regions from the 600-MHz 2Q spectrum of J2 are shown in Figure 2B. Note that whereas 128 direct peaks are expected in the ω_1 = 1′H + 2′H, 1′H + 2″H region (lower panel), only 64 remote peaks are expected in the ω_1 = 2′H + 2″H region (upper panel); the 2′H + 2″H remote peak region is much less crowded than the corresponding COSY, TOCSY, or 2Q direct peak region. One particular strength of the analysis of 1′H–2′H–2″H connectivities from 2Q spectra is that the ω_1 frequencies in the two distinct regins examined are not directly correlated; thus, signals from two or more spin subsystems that are overlapped in the direct peak region may be resolved in

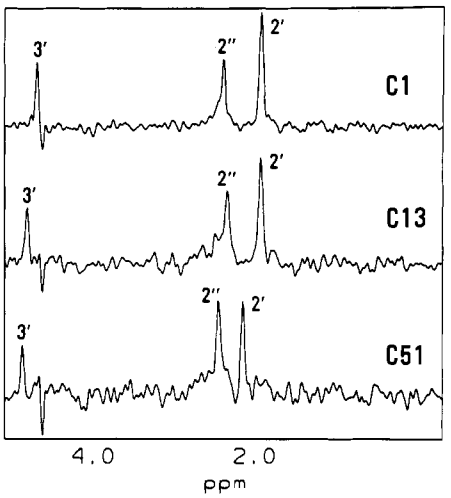

FIGURE 3: ω_1 cross sections at the 1'H resonance frequencies of C1, C13, and C51 from the 600-MHz TOCSY spectrum of J1, showing direct connectivities to 2'H and 2''H and relayed connectivities to 3'H. The solution was the same as that used for the 2Q spectrum in Figure 2. The spectrum was acquired at 37 °C with a 52-ms DIPSI-2 (Shaka et al., 1988) spin-locking period.

the remote peak region, and vice versa. An example is shown for G10 and G27 in Figure 2B, where at ω_2 = 5.33 ppm the direct peaks are overlapped but the remote peaks are fully resolved. A second important feature of the 2Q spectrum is that it is possible to identify the 2''H resonance frequencies, even though the 1'H + 2''H direct peak is usually absent from the spectrum (due to the small value of $J_{1'2''}$). The combination of 1'H + 2'H direct peak and 2'H + 2''H remote peak is sufficient to determine the 2''H resonance frequency: 1'H is determined directly from the ω_2 frequency; 2'H is identified by subtracting the 1'H frequency from the ω_1 frequency of the 1'H + 2'H direct peak; 2''H is identified by subtracting the 2'H frequency from the ω_1 frequency of the 2'H + 2''H remote peak. Analysis of these regions of the 2Q spectra has yielded 63 1'H-2'H-2''H spin *sub*systems for J1 and all 64 for J2. Tables listing the observed 2Q signals are available as supplementary material (see paragraph at end of paper regarding supplementary material).

The fourth stage of spin system identification in this study involves obtaining the assignments for the 3'H resonances. In theory, the 2Q spectra will exhibit a set of three connectivities for the 2'H-2''H-3'H spin *sub*system, in exact analogy to that described above for the 1'H-2'H-2''H spin *sub*system. In practice, the corresponding 3'H direct and remote peaks are much weaker due to passive couplings to 4'H and ^{31}P and because in typical B-form DNA conformations $^3J_{2'3'} < {}^3J_{1'2'}$ and $^3J_{2''3'} < {}^3J_{1'2''}$. For J1 and J2 only ~50% of the expected 2Q peaks are observed. Although the corresponding direct 2'H-3'H and 2''H-3'H connectivities are observed with much greater efficiency in TOCSY spectra, most of these TOCSY cross peaks are not resolved. Thus, the analysis of direct 2'H-3'H and 2''H-3'H scalar correlations proved not to be a viable option in either 2Q or TOCSY experiments. Ultimately, it was the observation of 1'H-3'H relayed connectivities in TOCSY spectra that provided the key information for assigning the 3'H resonances. A good compromise between sensitivity and efficiency of relayed coherence transfer is obtained for these HJs in TOCSY spectra with a 52-ms spin-lock period. A selection of ω_1 cross sections from the TOCSY spectrum of J1 acquired at 310 K with 52 ms of DIPSI-2 mixing are shown in Figure 3. Almost all of the 64 possible 1'H-3'H relayed connectivities are found in the 1'H-3'H region of the TOCSY spectra of J1 and J2, although in certain regions contour lines merge and the cross peaks are poorly resolved. These crowded regions can be partially deconvoluted by processing the data with resolution-enhancement functions and very high digital resolution. Additional 3'H assignments and verification of those made from relayed connectivities can be obtained from the connectivities that are observed in the 2Q spectrum and from 1'H-3'H and 6H/8H-3'H connectivities in NOESY spectra.

Sequence-Specific Assignments. The correlation of the sugar ring and base protons for each nucleotide and the assignment of these spin *sub*systems in a sequence-specific manner are based on characteristic short proton–proton distances identified in NOESY spectra (Wüthrich, 1986; van de Ven & Hilbers, 1988). The short-hand notation described by Wüthrich (1986) will be used to specify distances and corresponding NOEs.

Upon initial inspection of the NOESY spectra, it was quite clear that the extremely large number of cross peaks and corresponding severe spectral overlap would preclude a complete analysis of the characteristic regions of the spectrum that are normally utilized for obtaining sequential resonance assignments (6H/8H to 1'H, 2'H, and 2''H). Invariably, severe overlap is encountered, and it becomes impossible to resolve all of the expected intra- and interresidue connectivities. The strategy that proved successful for assigning the HJs was borrowed from the approach to obtain sequential assignments of protein ^{1}H NMR spectra, analyzing all potentially useful regions of the spectrum in parallel, circumventing problems in one region by finding resolved connectivities in another. As a result, a considerably greater effort is required than is typical for assigning duplex DNA. This involves obtaining spectra at two or more temperatures, identifying the exact coordinates of each peak observed in the spectra, and careful bookkeeping, again in parallel to the situation with proteins. The important NOE connectivities that are analyzed include the following: d_i(6,8;2',2''); d_s(2',2'';6,8); d_i(6,8;1'); d_s(1';6,8); d_i(Me;6); d_s(6,8;Me); d_i(6;5); d_s(6,8;5); d_i(5;2'); d_s(2',2'';5); d_s(5; Me); d_s(5;5). It was also useful to work on the two highly homologous junctions in parallel, not only for assigning the resonances from residues at and near the sites of sequence differences but also because the location and distribution of specific di-, tri-, and tetranucleotide sequences is changed. This facilitates the fitting of short segments of sequentially assigned residues to specific locations in the sequence. The remainder of this section is intended to give an overview of the protocol that was followed and is organized by residue type in relation to the ease in which the sequence-specific assignments could be obtained.

Figure 4 shows three expanded regions of connectivities in the 600-MHz NOESY spectrum of J2, to demonstrate the quality of the spectra observed and to show some of the useful NOE connectivities. The spectrum has been acquired with a 100-ms mixing time; thus, cross-peak intensities are affected by spin diffusion (Chazin et al., 1986). For example, the cross peaks corresponding to distances d_i(6,8;2'') and d_s(2';6,8) appear with relatively high intensity, despite the fact that these correspond to distances in excess of 3.5 Å (Wüthrich, 1986; van de Ven & Hilbers, 1988).

The assignment of the thymine residues in J1 and J2 is most easily obtained from the NOEs to the 5CH_3 resonances. The region containing connectivities between 6H and 8H base resonances and thymine methyl resonances of J2 is shown in Figure 4A. This is one of the most well-resolved portions of the spectrum due to the favorable dispersion of the methyl resonances, and all of the observed cross peaks could be as-

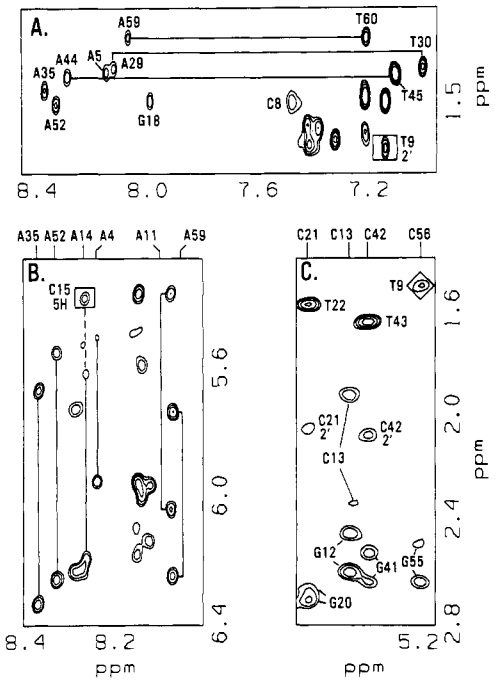

FIGURE 4: Expanded regions of the 600-MHz NOESY spectrum of 1 mM J2 acquired with a 100-ms mixing time at 37 °C. The buffer was as described in Figure 2. The ω_1 = T5CH$_3$, ω_2 = 6H,8H region (A), the ω_1 = 1′H,5H, ω_2 = A8H region (B), and part of the ω_1 = T5CH$_3$,2′H,2″H, ω_2 = C5H region (C) are shown with the sequence-specific assignments indicated in each panel. The cross peak in the box in (A) arises from a NOE between the 2′H and 6H resonances of T9, and horizontal lines connect a selected number of sequential (i,i−1) cross peaks to the corresponding intraresidue cross peak. In (B), the sequence-specific assignments of the well-resolved A8H resonances are indicated along the top, and a box is drawn around an A8H–C5H connectivity. In (C), the C5H resonances are identified along the top, and the CH$_3$, 2′H, and 2″H resonances are labeled at each cross peak. Note that the x and y axes of each panel are scaled independently for greater clarity in the presentation.

signed. These data provide sequential connectivities for all of the X-T sequences in J1 and J2 and serve as an excellent starting point for the sequence-specific assignment.

The key characteristic facilitating assignment of the adenine resonances is the favorable dispersion of the 8H signals. Figure 4B contains an expanded portion of the NOESY spectrum of J2 showing connectivities between the adenine 8H and 1′H resonances, with the intraresidue and sequential connectivities labeled for some of the cross peaks. Although the adenine signals are the most well resolved among the 6H/8H resonances, spectral crowding is clearly evident, in particular for A5, A28, A29, A40, and A54 at ω_2 ~8.15 ppm and for A14, A24, and A44 at ω_2 ~8.30 ppm. The sequential resonance assignments could be obtained for all of these adenine residues by careful analysis of the differences in the 8H chemical shifts in the NOESY spectra acquired at different temperatures, complemented by the comparative analysis of J1 and J2.

Among the standard 6H/8H connectivities, the cytosine 6H cross peaks are the most difficult to identify because they have wide ω_2 profiles, the result of the scalar coupling to the 5H protons. The intraresidue and sequential connectivities between C5H and 2′H and 2″H resonances and between C5H and thymine 5CH$_3$ resonances are very powerful alternative routes to the standard 6H pathways for assignment of X-C and C-T sequences, respectively. A selected number of examples labeled with the sequence-specific assignment are given in Figure 4C. The advantage of using NOEs to the 5H resonances for obtaining assignments is that these signals are fairly well dispersed and relatively isolated from the rest of the spectrum, having only limited overlap with a subset of the 1′H resonances. The d_s(6,8;5) connectivities have also proven to be useful as a means for assigning X-C sequences. The assignment of these cross peaks is facilitated by the presence of the d_i(5;6) cross peak which provides an internal reference for both the chemical shift and the ω_1 and ω_2 cross-peak profiles and because there are only 17 X-C sequences in each of the HJs. An example is shown in Figure 4B, wherein the cross peak for the sole A-C sequence in J2 is highlighted by a box drawn around the cross peak.

The basic strategy for the sequence-specific assignment of the guanine resonances was the same as that for the adenines. However, the guanine assignments were much more difficult to obtain because the G8H resonances have a much smaller spectral dispersion than the A8H resonances and many of the corresponding cross peaks are only poorly resolved. Processing of the NOESY spectra with resolution-enhancement functions and very high digital resolution (ω_1 = 2.5 Hz/pt, ω_2 = 1.2 Hz/pt) was critical to the success in making the guanine sequential assignments. Also, by assigning as many of the other residues as possible first, NOEs to the sequential neighbors could be used to assist in identifying the cross peaks to the G8H resonances. Five examples are identified in Figure 4, including the G18–T19 cross peak in panel A and the G12–C13, G20–C21, G41–C42, and G55–C56 cross peaks in panel C.

Concluding Remarks

With the methodology described above, it has been possible to obtain virtually complete assignments for the 1′H, 2′H, 2″H, and 3′H sugar ring protons and for the nonlabile base protons of J1 and J2. NMR studies of the labile amino and imino base protons have also been carried out and indicate base pairing up to and including the junction in both J1 and J2. Our results are in agreement with the earlier study of Wemmer et al. (1985). A full report on these results will be presented in a subsequent paper, when spectral analysis is completed.

We note that some of the ^{1}H resonances of residues at the junction are broadened in both J1 and J2. The effect appears to be temperature dependent because these lines sharpen somewhat as the temperature is lowered from 37 to 27 °C. A likely explanation for these broadening effects is melting out of the base pairs at the junction at these "high" temperatures, resulting in conformational heterogeneity. Further studies are underway in this laboratory in an attempt to clarify the origin of this effect.

The sequence-specific assignments will permit further analysis of the available NMR data in terms of the implications concerning junction structure and dynamics. Some cross-strand NOEs have been identified that are indicative of the nature of the packing of the arms of the HJ structure and, correspondingly, of the geometry of the junction. For example, in the 5H to methyl region of the NOESY spectrum of J2, a nonsequential NOE between T9 and C56 is readily identified (Figure 4C), whereas the corresponding NOE in J1 is clearly not present. This represents primary *direct* evidence for differences in the structures of J1 and J2, although further experimental evidence is required to distinguish among the various structural models for the Holliday junction. We refrain from a more detailed interpretation here since virtually all of our efforts to date have centered on obtaining full sequential assignments to ensure that the additional nonsequential data can be interpreted unambiguously. Our detailed analysis of the results from studies of HJ structure and dynamics should provide important information for understanding the role of Holliday junctions in genetic recombination and repair.

ACKNOWLEDGMENTS

We thank Dr. Matthew Kalnick for suggesting the titration of oligonuclotide single strands by ^{1}H NMR, Dr. Mark Rance for continued support with experimental methodology, and Beth Larson for help with typing the manuscript.

SUPPLEMENTARY MATERIAL AVAILABLE

Two tables listing 1′H-2′H-2″H direct and remote peaks observed at ω_2 = 1′H for J1 and J2 (4 pages). Ordering information is given on any current masthead page.

REFERENCES

Bax, A., & Davis, D. G. (1985) *J. Magn. Reson. 65*, 355–360.
Braunschweiler, L., & Ernst, R. R. (1983) *J. Magn. Reson. 53*, 521–528.
Braunschweiler, L., Bodenhausen, G., & Ernst, R. R. (1983) *Mol. Phys. 48* (3), 535–560.
Chazin, W. J., Wüthrich, K., Hyberts, S., Rance, M., Denny, W. A., & Leupin, W. (1986) *J. Mol. Biol. 190*, 439–453.
Churchill, M. E. A., Tullius, T. D., Kallenbach, N. R., & Seeman, N. C. (1988) *Proc. Natl. Acad. Sci. U.S.A. 85*, 4653–4656.
Cooper, J. P., & Hagerman, P. J. (1987) *J. Mol. Biol. 198*, 711–719.
Davis, D. G. (1989) *J. Magn. Reson. 81*, 603–607.
Diekmann, S., & Lilley, D. M. J. (1989) *Nature 341*, 763–766.
Duckett, D. R., Murchie, A. I. H., Diekmann, S., Kitzing, E., Kemper, B., & Lilley, D. M. J. (1988) *Cell 55*, 79–89.
Furlong, J. C., & Lilley, D. M. J. (1986) *Nucleic Acids Res. 14*, 3995–4007.
Gough, G. W., & Lilley, D. M. J. (1985) *Nature 313*, 154–156.
Gough, G. W., Sullivan, K. M., & Lilley, D. M. J. (1986) *EMBO J. 5*, 191–196.
Grütter, R., Otting, G., Wüthrich, K., & Leupin, W. (1988) *Eur. Biophys. J. 16*, 279–286.
Holliday, R. (1964) *Genet. Res. 5*, 282–304.
Kallenbach, N. R., Ma, R. I., & Seeman, N. C. (1983) *Nature 305*, 829–831.
Levitt, M., & Freeman, R. (1979) *J. Magn. Reson. 33*, 473–476.
Macura, S., & Ernst, R. R. (1980) *Mol. Phys. 41*, 95–117.
Marion, D., & Wüthrich, K. (1983) *Biochem. Biophys. Res. Commun. 113*, 967–974.
Marky, L. A., Kallenbach, N. R., McDonough, K. A., & Seeman, N. C. (1987) *Biopolymers 26*, 1621–1634.
Mueller, J. E., Kemper, B., Cunningham, R. P., Kallenbach, N. R., & Seeman, N. C. (1988) *Proc. Natl. Acad. Sci. U.S.A. 85*, 9441–9445.
Muller, B., Jones, C., Kemper, B., & West, S. C. (1990) *Cell 60*, 329–336.
Murchie, A. I. H., Clegg, R. M., Kitzing, E. V., Duckett, D. R., Diekmann, S., & Lilley, D. M. J. (1989) *Nature 341*, 763–766.
Otting, G., Grütter, R., Leupin, W., Minganti, C., Ganesh, K. N., Sproat, M. J., & Wüthrich, K. (1987) *Eur. J. Biochem. 166*, 215–220.
Parsons, C. A., Murchie, A. I., Lilley, D. M., & West, S. C. (1989) *EMBO J. 8*, 239–246.
Patel, D. J., Shapiro, L., & Hare, D. (1987) *Annu. Rev. Biophys. Biophys. Chem. 16*, 423–454.
Plateau, P., & Gueron, M. J. (1982) *J. Am. Chem. Soc. 104*, 7310–7311.
Rance, M. (1987) *J. Magn. Reson. 74*, 557–564.
Reid, B. R. (1987) *Q. Rev. Biophys. 20*, 1–34.
Seeman, N. C. (1982) *J. Theor. Biol. 99*, 237–247.
Seeman, N. C., & Kallenbach, N. R. (1983) *Biophys. J. 44*, 201–209.
Shaka, A. J., Lee, C. J., & Pines, A. (1988) *J. Magn. Reson 77*, 274–293.
Sigal, N., & Alberts, B. (1972) *J. Mol. Biol. 71*, 789–793.
van de Ven, F. J. M., & Hilbers, C. W. (1988) *Eur. J. Biochem. 178*, 1–38.
Wemmer, D. E., & Reid, B. R. (1985) *Annu. Rev. Phys. Chem. 36*, 105–137.
Wemmer, D. E., Wand, A. J., Seeman, N. C., & Kallenbach, N. R. (1985) *Biochemistry 24*, 5745–5749.
Whitehouse, H. L. K. (1982) *Genetic Recombination: Understanding the Mechanism*, Wiley, New York.
Wüthrich, K. (1986) *NMR of Proteins and Nucleic Acids*, Wiley, New York.